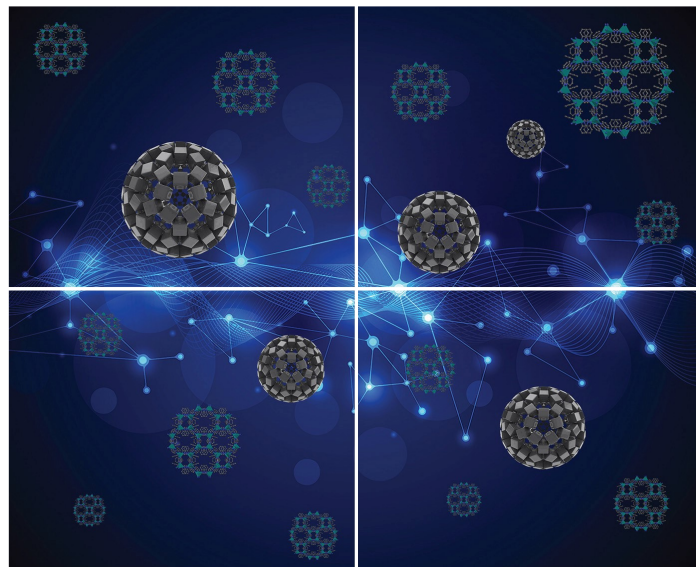


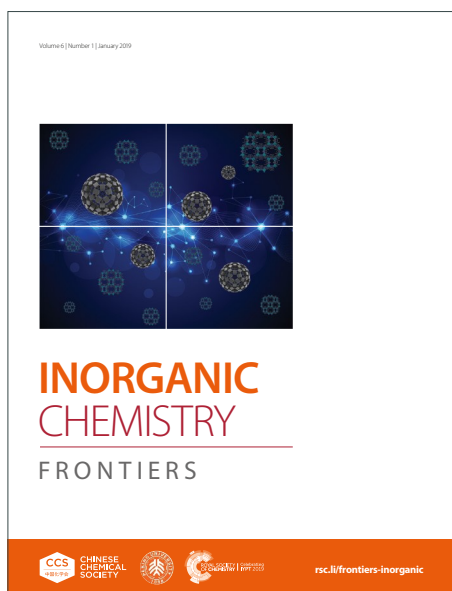
INORGANIC CHEMISTRY

FRONTIERS

Accepted Manuscript



This article can be cited before page numbers have been issued, to do this please use: X. Zeng, Z. Wang, M. He, W. Lu, W. Huang, B. An, J. Li, L. Mufan, B. Spencer, S. Day, F. Tuna, E. J. L. McInnes, M. Schroder and S. Yang, *Inorg. Chem. Front.*, 2024, DOI: 10.1039/D4QI02225D.



This is an Accepted Manuscript, which has been through the Royal Society of Chemistry peer review process and has been accepted for publication.

Accepted Manuscripts are published online shortly after acceptance, before technical editing, formatting and proof reading. Using this free service, authors can make their results available to the community, in citable form, before we publish the edited article. We will replace this Accepted Manuscript with the edited and formatted Advance Article as soon as it is available.

You can find more information about Accepted Manuscripts in the [Information for Authors](#).

Please note that technical editing may introduce minor changes to the text and/or graphics, which may alter content. The journal's standard [Terms & Conditions](#) and the [Ethical guidelines](#) still apply. In no event shall the Royal Society of Chemistry be held responsible for any errors or omissions in this Accepted Manuscript or any consequences arising from the use of any information it contains.

ARTICLE

A novel cerium-based metal-organic framework supported Pd catalyst for semi-hydrogenation of phenylacetylene

Xiangdi Zeng,^a Zi Wang,^a Meng He,^a Wanpeng Lu,^a Wenyuan Huang,^b Bing An,^a Jiangnan Li,^b Mufan Li,^b Ben F. Spencer,^c Sarah J. Day,^d Floriana Tuna,^{a,e} Eric J. L. McInnes,^a Martin Schröder^{a*} and Sihai Yang^{a,b*}

Received 00th January 20xx,
Accepted 00th January 20xx

DOI: 10.1039/x0xx00000x

Phenylacetylene is a detrimental impurity in the polymerisation of styrene, capable of poisoning catalysts even at ppm levels and significantly degrading the quality of polystyrene. The semi-hydrogenation of phenylacetylene to styrene instead of ethylbenzene is, therefore, an important industrial process. We report a novel cerium(IV)-based metal-organic framework (denoted as Ce-bptc), which is comprised of {Ce₆} clusters bridged by biphenyl-3,3',5,5'-tetracarboxylate linkers. Ce-bptc serves as an ideal support for palladium nanoparticles and the Pd@Ce-bptc catalyst demonstrates an excellent catalytic performance for semi-hydrogenation of phenylacetylene, achieving a selectivity of 93% to styrene on full conversion under ambient conditions with excellent reusability. *In situ* synchrotron X-ray powder diffraction and electron paramagnetic resonance spectroscopy revealed the binding domain of phenylacetylene within Ce-bptc and details of the reaction mechanism.

Introduction

Phenylacetylene is a key impurity that harms the polymerisation of styrene; even concentrations of just a few dozen ppm can poison the catalyst and significantly degrade the quality of polystyrene.¹ Therefore, semi-hydrogenation of phenylacetylene to styrene, rather than the undesired ethylbenzene, is of great importance to the polystyrene industry.² Palladium metal nanoparticles is the leading catalyst for this reaction.^{3,4} To maximise the utilisation of noble metals and stabilise Pd nanoparticles, doping them into porous materials, such as zeolites, carbons and metal-organic frameworks (MOFs), has been investigated.⁵⁻¹¹ In this context, the porous supports have notable impacts on the catalytic activity of Pd nanoparticles and MOFs have received much attention due to their high structural diversity and tuneability.⁵ For example, sandwiched Pd nanoparticles supported on UiO-series MOFs have shown an exceptional TOF (turnover frequency) of 13,835 h⁻¹.⁹ The hydrophobicity of the ligand on the porous material can also influence the catalytic activity of Pd nanoparticles. It has been reported that the functional group

on the pore surface can promote the charge transfer between the porous support and Pd sites, giving rise to an increased catalytic performance.^{9,11} Additionally, the metal centres in MOFs can also influence the catalytic microenvironment. Compared with Zr-based MOFs⁹, Ce-based MOFs often contain both Ce(III)/Ce(IV) sites, which can act as a redox couple. Thus, Ce-MOFs can promote charge transfer to facilitate various redox reactions,¹²⁻¹⁴ and act as excellent catalyst support for semi-hydrogenation reactions.

Herein, we report a novel Ce(IV)-based MOF (Ce-bptc), consisting of {Ce₆} clusters bridged by biphenyl-3,3',5,5'-tetracarboxylate linkers. Pd nanoparticles supported on Ce-bptc affords an efficient catalyst Pd@Ce-bptc for semi-hydrogenation of phenylacetylene, yielding a selectivity of 93% to styrene on full conversion under ambient conditions. The catalytic mechanism has been elucidated by *in situ* synchrotron X-ray powder diffraction (SXPD), X-ray photoelectron spectroscopy (XPS), and electron paramagnetic resonance (EPR) spectroscopy.

Results and discussion

Microcrystalline Ce-bptc sample was synthesised by solvothermal reaction of (NH₄)₂Ce(NO₃)₆ and biphenyl-3,3',5,5'-tetracarboxylic acid (H₄bptc). Rietveld refinement of high resolution SXPD data of Ce-bptc {Ce₆O₄(OH)₄(bptc)₃·(H₃O)_{1.6}·3DMF·10H₂O} revealed that the crystal structure is comprised of twelve-connected {Ce₆O₄(OH)₄(CO₂)₁₂} clusters, which are bridged by tetracarboxylate ligands to form an open and neutral framework in the *ftw* topology^{15,16} (Figure 1a, Table S1).

^a Department of Chemistry, University of Manchester, Manchester, M13 9PL, UK. M.Schroder@manchester.ac.uk

^b College of Chemistry and Molecular Engineering, Beijing National Laboratory for Molecular Sciences, Peking University, Beijing, 100871, China. Sihai.Yang@pku.edu.cn

^c Department of Materials, The University of Manchester, Manchester, M13 9PL, UK.

^d Diamond Light Source, Harwell Science Campus, Didcot, Oxfordshire, OX11 0DE, UK.

^e Photon Science Institute, University of Manchester, Manchester, M13 9PL, UK.

* Supplementary Information available: CCDC 2205374 and 2205379. See DOI: 10.1039/x0xx00000x



Six Ce(IV) atoms are assembled into an octahedron, where the eight faces are occupied by $\mu_3\text{-O}^{2-}$ or $\mu_3\text{-OH}^-$ groups in each $\{\text{Ce}_6\text{O}_4(\text{OH})_4(\text{CO}_2)_{12}\}$ cluster. Each Ce(IV) atom is coordinated to eight O atoms, four of which belong to four different bptc^{4-} ligands and the remaining four are from $\mu_3\text{-O}^{2-}/\text{OH}^-$ groups. Each bptc^{4-} ligand is connected to four different $\{\text{Ce}_6\}$ clusters with each carboxylate coordinated by two adjacent Ce(IV) atoms in the same cluster in a bi-monodentate mode. Ce-bptc shows cubic cages with $\{\text{Ce}_6\}$ clusters on the vertices and planar

bptc^{4-} linker on the faces (Figure 1b). The cubic cages have a dimension of $\sim 9.4 \text{ \AA}$ and are interconnected through smaller tetrahedral cages (dimension of $\sim 3.5 \text{ \AA}$) located at the twelve edges of the cubic cages (Figure 1c). Thermogravimetric analysis (TGA) shows that Ce-bptc is stable up to *ca.* 250 °C before decomposition (Figure S10).

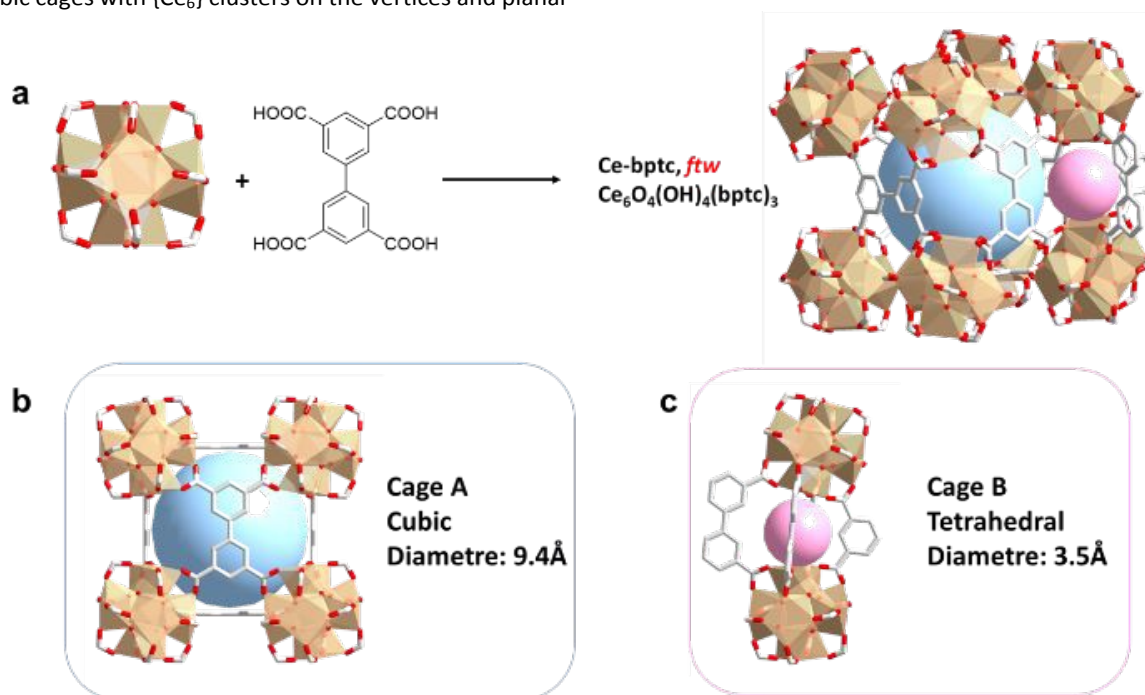


Figure 1 Crystal structure of Ce-bptc. (a) Views of $\{\text{Ce}_6\}$ cluster, linker and caged structure of Ce-bptc. (b) Detailed view of cage A (cubic cage). (c) Detailed view of cage B (tetrahedral cage). Colour code: Ce, light brown; C, grey; O, red; H, omitted for clarity. Cage A and Cage B are highlighted by blue and pink spheres, respective

To encapsulate Pd nanoparticles, Pd precursors (0.3, 2.0, 3.7 and 5.4 wt%) were first dissolved in water and then embedded within Ce-bptc using a double solvent method¹⁷, followed by treatment under a flow of H_2 at 150 °C for 2 hours to yield Pd@Ce-bptc, which shows retention of the framework structure of Ce-bptc as confirmed by powder X-ray diffraction (PXRD, Figure 2a, S1). No obvious Bragg peaks of Pd nanoparticles or PdO_x were observed, indicating the excellent dispersion of Pd species in Ce-bptc. The diffuse reflectance infrared Fourier transform spectra (DRIFTS) of Ce-bptc and Pd@Ce-bptc indicate the retention of the structure and stretching mode of $\mu_3\text{-OH}^-$ groups upon Pd doping (Figure 2b). The encapsulation of Pd nanoparticles in Ce-bptc is also accompanied by a reduction of the Brunauer-Emmett-Teller (BET) surface area from 532 to 390 $\text{m}^2 \text{ g}^{-1}$ (Ce-bptc and Pd@Ce-bptc, respectively; Figure S3). Scanning electron microscopy (SEM) and energy dispersive X-Ray (EDX) analysis show that Pd nanoparticles are distributed homogeneously in the MOF (Figures S7-S8). For comparison, we also prepared another benchmark MOF, Ce-UiO-66¹², which shows reduced crystallinity and almost nil porosity upon the encapsulation of Pd (Figure S2, S9).

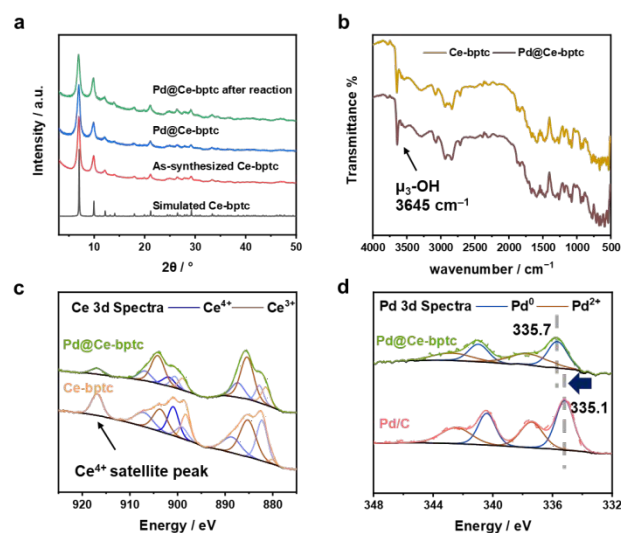


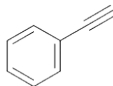
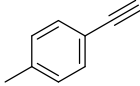
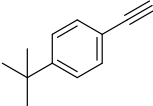
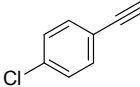
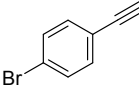
Figure 2 (a) PXRD patterns of the simulated Ce-bptc, as-synthesized Ce-bptc, and Pd@Ce-bptc before and after reaction. (b) DRIFT spectra of Ce-bptc and Pd@Ce-bptc. (c) XPS Ce 3d spectra of Ce-bptc and Pd@Ce-bptc. (d) XPS Pd 3d spectra of Pd@Ce-bptc and Pd/C.



XPS experiments were conducted to study the electronic state of Ce and Pd sites (Figure 2c,d). The Ce 3d spectra were decomposed according to well-established peak models¹⁸ it was found that both Ce(IV) and Ce(III) species (73.4% and 26.6%, respectively) exist in Ce-bptc, which is consistent with other reported Ce(IV)-based MOFs.¹⁹ Upon the reduction, the Ce(IV) satellite peak at 916.8 eV decreased significantly, and the ratio of Ce(III) increased from 26.6% to 62.1%, while the increased amount of Ce(III) can facilitate the electron transfer. To investigate the interactions between the Pd nanoparticles

and MOF host, the Pd 3d XPS spectra of Pd@Ce-bptc and Pd/C were measured (Figure 2d). The Pd 3d_{5/2} peak for Pd@Ce-bptc was located at 335.7 eV (calibrated by C1s = 284.8 eV). Compared with the Pd 3d_{5/2} peak of Pd/C (335.1 eV),²⁰ Pd@Ce-bptc was found at higher Binding Energy, indicating promoted electron transfer from Pd to Ce in Pd@Ce-bptc.²¹ This shift in Binding Energy for Pd 3d_{5/2} is not due to issues with charge calibration as other peak positions are at expected values after calibration.

Table 1 Summary of catalytic activity of semi-hydrogenation of alkynes to alkenes

Catalyst	Substrate	Time (hrs)	Conv. (%)	Sel. of alkene (%)
Pd@Ce-bptc-2.0%		2.5	>99	93
powdered mixture of 2%Pd/C+Ce-bptc		2.5	>99	45
Pd@Zr-bptc-2.2%		2.5	>99	91
Pd@Ce-UiO-66-2.0%		3	>99	88
Pd@Zr-UiO-66-2.1%		6	>99	85
Pd@CeO ₂ -2.0%		2.5	>99	71
Pd@ZrO ₂ -2.1%		2.5	>99	17
2%Pd/C		2.5	>99	10
Ce-bptc		2.5	0	0
Pd@Ce-bptc-2.0%		1.0	52	99
Pd@Ce-bptc-2.0%			1.0	55
Pd@Ce-bptc-2.0%		1.0	85	89
Pd@Ce-bptc-2.0%		1.0	42	86
Pd@Ce-bptc-2.0%		1.0	20	90

Reaction conditions: 5mg catalyst, 1 mmol substrate, 1 mmol mesitylene as internal standard, 2 mL THF, 25°C water bath, 1 bar H₂ balloon.



The catalytic performance of a range of Pd-based catalysts (Pd@Ce-bptc, Pd@Zr-bptc, Pd@Ce-Uio-66, Pd@Zr-Uio-66, Pd@CeO₂, Pd@ZrO₂) were tested for the semi-hydrogenation of phenylacetylene (Figure S12). Firstly, the impact of different loadings of Pd nanoparticles (0.3, 2.0, 3.7 and 5.4%) in Pd@Ce-bptc was studied. At 25 °C and under 1 bar of H₂ for 1 hour, the conversion of phenylacetylene increased from 33% to 91% upon increased loading of Pd nanoparticles, and the TOF decreased from 2385 to 362 h⁻¹ (Figure 3a). To balance the TOF and conversion, Pd@Ce-bptc with 2.0 wt% of Pd was used for further tests and comparison with other catalysts.

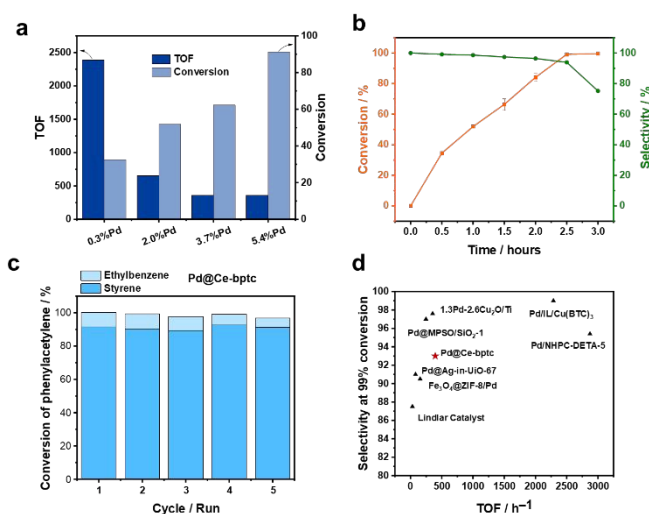


Figure 3 Studies of catalytic performance. Reaction conditions: 5 mg MOF catalyst, 1 mmol phenylacetylene, 1 mmol mesitylene, 2 mL THF, 25°C, 2.5 hours. (a) Conversion of phenylacetylene and selectivity of styrene on Pd@Ce-bptc with different Pd loading. (b) Conversion of phenylacetylene and selectivity of styrene on Pd@Ce-bptc-2.0% over time. (c) The cycle test of Pd@Ce-bptc. (d) The catalytic performance comparison of different Pd nanoparticles loaded catalysts under 1 bar H₂ reaction condition.

For the reaction at 25 °C and 1 bar of H₂ for 2.5 hours, Pd@Ce-bptc-2.0% shows a selectivity of 93% to styrene on full conversion of phenylacetylene (Figure 3b). Control experiments with Pd/C (Pd supported on carbon black) demonstrate >99% conversion with only 10% selectivity to styrene (the major product is ethylbenzene), while bare Ce-bptc showed nil activity (Table 1). A powdered mixture of 2% Pd/C and Ce-bptc showed a selectivity of 45% to styrene on full conversion, demonstrating the important role of confinement of Pd nanoparticles in the pores to promote the semi-hydrogenation instead of full hydrogenation. The selectivity of Pd@Ce-bptc-2.0% is better than the commercial Lindlar catalyst (selectivity of 87% on full conversion) and other supported Pd catalysts on both MOFs

(namely Pd@Ce-Uio-66, Pd@Zr-bptc, Pd@Zr-Uio-66) and metal oxide (Pd@CeO₂ and Pd@ZrO₂) with the Pd loading of 2 wt% (Table 1). To explore the reusability, used Pd@Ce-bptc was tested for 5 consecutive runs, and the conversion of phenylacetylene retained 97%. After 5 consecutive runs, the PXRD pattern of the used catalyst did not show any obvious change, demonstrating its high stability (Figure 3c, Figure S14). In comparison, the conversion over Pd@Zr-bptc decreased from 98% to 88% after 5 runs (Figure S15). The improved stability of Pd@Ce-bptc compared with Pd@Zr-bptc is consistent with the XPS result, which shows stronger interaction between Pd nanoparticles and Ce-bptc (Figure 2d, S12).

The semi-hydrogenation of phenylacetylene-based substrates with various para-substitution were tested over Pd@Ce-bptc to investigate the impact of substitution groups on the reaction (Table 1). The reaction time for all substrates is set at 1 hour, and the conversion of 4-methylphenylacetylene, 4-*tert*-butylphenylacetylene, 4-chlorophenylacetylene and 4-bromophenylacetylene is 55%, 85%, 42% and 20%, respectively (Figure S16-20). The results suggest that the substrate with an electron-donating group shows higher conversion compared with phenylacetylene, while the substrate with an electron-withdrawing group shows lower conversion. Overall, these results suggest that Pd@Ce-bptc is a highly active and stable catalyst for semi-hydrogenation at room temperature.

To investigate the host-guest interaction between adsorbed substrate and Ce-bptc, SXPD data was collected for phenylacetylene-loaded Ce-bptc, and highly satisfactory Rietveld refinement revealed the binding domains (Figure 4a, S20, Table S1). The ethynyl group of adsorbed phenylacetylene molecules interact with the bridging oxygen and carboxylate oxygen centres on the {Ce₆O₆} clusters to form hydrogen bonds [C≡C-H...O_{bridge} = 3.46(5) Å, C≡C-H...O_{ligand} = 3.15(8) Å]. These adsorbed molecules are further stabilised by parallel-displaced π...π interactions between the C≡C bond/benzene rings of guest molecules and ligands of Ce-bptc with an inter-planar distance of 4.02(1) Å and 4.09(1) Å, respectively. Thus, the SPXRD study confirms the notable host-guest binding interactions that accelerated the charge transfer and thus promoted the hydrogenation efficiency.^{22,23}

It is reported that the hydrogenation of phenylacetylene to styrene and ethylbenzene could proceed *via* two different mechanisms: one-pathway or two-pathway.²⁴ One-pathway mechanism involves the direct hydrogenation of the triple bond to a single bond, while two-pathway mechanism undergoes a two-step hydrogenation process, which involves the formation of single or multiple adsorbed species, similar to the semihydrogenation of acetylene.^{25,26} Given the high selectivity to styrene observed over Pd@Ce-bptc, it is evident that the reaction predominantly follows the two-pathway mechanism involving adsorbed intermediates.



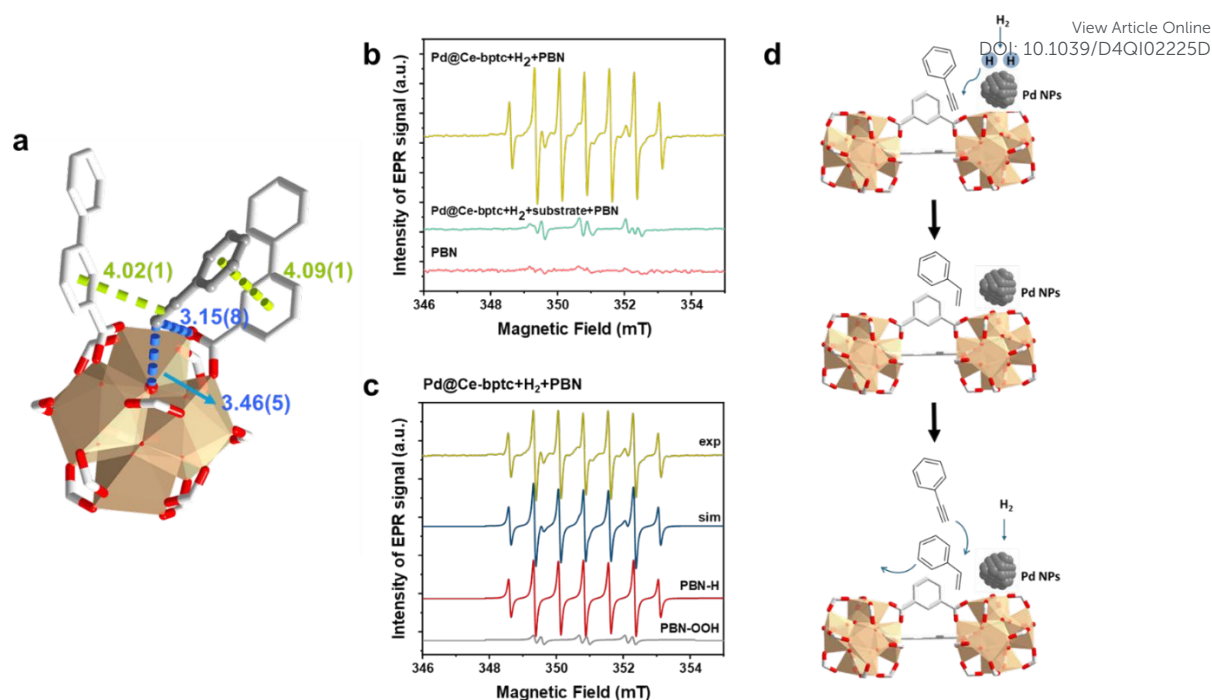


Figure 4. Studies of catalytic mechanism. (a) Views of crystal structure of phenylacetylene-loaded Ce-bptc. All models were obtained from Rietveld refinements of SXPD data. The guest molecules are highlighted by using amplified ball-and-stick model, hydrogen atoms are omitted for clarity. Bond distances are in angstrom. (b) *In situ* X-band EPR spectra under controlled conditions using PBN as a spin trap reagent. Pd@Ce-bptc + H₂ + THF; Pd@Ce-bptc + H₂ + phenylacetylene + THF; PBN (THF solution). (c) Experimental and simulated spectra of the lime line in (b), showing a major component, PBN-H (red, simulation), and a minor component, PBN-OOH (grey, simulation). (d) The proposed reaction mechanism of phenylacetylene semihydrogenation reaction (NPs = nanoparticles).

To identify any radical species in this reaction, *in situ* EPR spin-trapping experiments were conducted. Considering the transient nature of many free radicals, with lifetimes significantly shorter than the acquisition time of EPR spectra, N-tert-Butyl- α -phenylnitron (PBN) was employed as a spin trap reagent²⁷ to identify radicals as long-lived PBN-radical adducts. When H₂ and the catalyst were present in the reaction solution, an intense seven-line EPR signal with a *g*-factor of 2.0055 and hyperfine coupling constants $A^N = 15.0$ G and $A^{H1} = A^{H2} = 7.4$ G was detected. This signal is unequivocally attributed to the PBN-H radical²⁸, indicating that H₂ is activated directly by the confined Pd nanoparticles, leading to the homolytic dissociation of the H-H bond and the generation of H \cdot radicals (Figure 4b,4c, Table S2). Interestingly, no PBN signal was observed when the substrate was added to the reaction solution, suggesting that the hydrogenation involving H \cdot radicals and the substrate is extremely rapid, preventing H \cdot radicals from being trapped by PBN (Figure S22). Thus, the EPR study confirms the reaction pathway (Figure 4d): H₂ is firstly activated by the Pd nanoparticles, resulting in the homolytic dissociation of the H-H bond and the release of H \cdot radicals, which subsequently attack the C=C bond of adsorbed phenylacetylene, forming the desired product, styrene, which can readily desorb from the adsorption site in competitive adsorption with phenylacetylene, thus avoiding the over-hydrogenation to ethylbenzene.

Conclusions

In summary, we report a novel cerium(IV)-based MOF, Ce-bptc, which is comprised of {Ce₆O₄(OH)₄(CO₂)₁₂} clusters that are further bridged by tetracarboxylate ligands to afford an open framework in *ftw* topology. Encapsulation of Pd nanoparticles gives a highly efficient Pd@Ce-bptc catalyst, which exhibited an excellent catalytic performance in the semihydrogenation of phenylacetylene, achieving a selectivity of 93% to styrene on full conversion at 25 °C and 1 bar H₂. The molecular details of host-guest interactions between adsorbed substrate and MOF host were investigated by SXPD analysis. *In situ* EPR study revealed the mechanism of H₂ splitting and rapid hydrogenation *via* H \cdot radicals. This study highlights the great potential of Ce-based MOFs as catalyst support for semihydrogenation reactions, offering advantages in selectivity over traditional supports based upon metal oxides.

Author Contribution

XZ, WL, WH, BA, JL and ML: synthesis and characterisation of materials, catalysis testing and data analysis; ZW, FT and EJLM: collection and analysis of EPR data; MH and SJD: collection and analysis of synchrotron X-ray diffraction data; BFS: collection and analysis of XPS data; MS and SY: overall direction of the project; XZ, MS and SY: preparation of the manuscript with contributions from all authors.



Conflicts of interest

The authors declare no conflicts of interest.

Data availability

The data supporting this article have been included as part of the ESI.† Crystallographic data have been deposited at the CCDC under CCDC 2205374 and 2205379† and can be obtained from <https://doi.org/10.1039/x0xx00000x>.

Acknowledgements

We thank EPSRC (EP/I011870, EP/V056409, EP/W014521/1), University of Manchester, National Science Foundation of China and BNLMS for funding. This project has received funding from the European Research Council (ERC) under the European Union's Horizon 2020 research and innovation programme (grant agreement No 742401, NANO-CHEM and PoC665632). We thank Diamond Light Source for access to Beamline I11.

Notes and references

- 1 Y. Liu, W. Guo, X. Li, P. Jiang, N. Zhang, M. Liang, Copper Single-Atom-Covered Pt Nanoparticles for Selective Hydrogenation of Phenylacetylene, *ACS Appl. Nano Mater.* 2021, **5**, 5292-5300.
- 2 L. Yang, Y. Jin, X. Fang, Z. Cheng, Z. Zhou, Magnetically Recyclable Core-Shell Structured Pd-Based Catalysts for Semihydrogenation of Phenylacetylene, *Ind. Eng. Chem. Res.* 2017, **48**, 14182-14191.
- 3 M. Crespo-Quesada, F. Cárdenas-Lizana, A.-L. Dessimoz, L. Kiwi-Minsker, Modern Trends in Catalyst and Process Design for Alkyne Hydrogenations, *ACS Catal.* 2012, **8**, 1773-1786.
- 4 S. A. Nikolaev, L. N. Zhanavskina, V. V. Smirnov, V. A. Averyanov, K. L. Zhanavskina, Catalytic hydrogenation of alkyne and alkadiene impurities from alkenes. Practical and theoretical aspects, *Russ. Chem. Rev.* 2009, **3**, 231-247.
- 5 Q. Yang, Q. Xu, H.-L. Jiang, Metal-organic frameworks meet metal nanoparticles: synergistic effect for enhanced catalysis, *Chem. Soc. Rev.* 2017, **46**, 4774-4808.
- 6 J. Zhang, L. Wang, Y. Shao, Y. Wang, B. C. Gates, F.-S. Xiao, A Pd@ zeolite catalyst for nitroarene hydrogenation with high product selectivity by sterically controlled adsorption in the zeolite micropores, *Angew. Chem. Int. Ed.* 2017, **56**, 9747-9751.
- 7 H. Q. Wu, L. Huang, J. Q. Li, A. M. Zheng, Y. Tao, L. X. Yang, W. H. Yin, F. Luo, Pd@ Zn-MOF-74: Restricting a Guest Molecule by the Open-Metal Site in a Metal-Organic Framework for Selective Semihydrogenation, *Inorg. Chem.* 2018, **20**, 12444-12447.
- 8 L. Chen, B. Huang, X. Qiu, X. Wang, R. Luque, Y. Li, Seed-mediated growth of MOF-encapsulated Pd@ Ag core-shell nanoparticles: toward advanced room temperature nanocatalysts, *Chem. Sci.* 2016, **1**, 228-233.
- 9 K. Choe, F. Zheng, H. Wang, Y. Yuan, W. Zhao, G. Xue, X. Qiu, M. Ri, X. Shi, Y. Wang, G. Li, Z. Tang, Fast and selective semihydrogenation of alkynes by palladium nanoparticles sandwiched in metal-organic frameworks, *Angew. Chem. Int. Ed.* 2020, **9**, 3650-3657.
- 10 L. Li, W. Yang, Q. Yang, Q. Guan, J. Lu, S.-H. Yu, H.-L. Jiang, Accelerating chemo- and regioselective hydrogenation of alkynes over bimetallic nanoparticles in a metal-organic framework, *ACS Catal.* 2020, **14**, 7753-7762.
- 11 M. Guo, Q. Meng, W. Chen, Z. Meng, M.-L. Gao, Q. Li, X. Duan, H.-L. Jiang, Dual microenvironment modulation of Pd nanoparticles in covalent organic frameworks for semihydrogenation of alkynes, *Angew. Chem. Int. Ed.* 2023, **62**, e202305212.
- 12 J. Jacobsen, A. Ienco, R. D'Amato, F. Costantino and N. Stock, The chemistry of Ce-based metal-organic frameworks, *Dalton Trans.* 2020, **49**, 16551-16586.
- 13 M. Lammert, M. T. Wharmby, S. Smolders, B. Bueken, A. Lieb, K. A. Lomachenko, D. D. Vos and N. Stock, Cerium-based metal organic frameworks with UiO-66 architecture: synthesis, properties and redox catalytic activity, *Chem. Commun.* 2015, **51**, 12578-12581.
- 14 X. He, B. G. Looker, K. T. Dinh, A. W. Stubbs, T. Chen, R. J. Meyer, P. Serna, Y. Román-Leshkov, K. M. Lancaster, M. Dincă, Cerium (IV) enhances the catalytic oxidation activity of single-site Cu active sites in MOFs, *ACS Catal.* 2020, **14**, 7820-7825.
- 15 H. Wang, X. Dong, J. Lin, S. J. Teat, S. Jensen, J. Cure, E. V. Alexandrov, Q. Xia, K. Tan, Q. Wang, D. H. Olson, D. M. Proserpio, Y. J. Chabal, T. Thonhauser, J. Sun, Y. Han, J. Li, Topologically guided tuning of Zr-MOF pore structures for highly selective separation of C6 alkane isomers, *Nat. Commun.* 2018, **9**, 1745.
- 16 J. Li, G. L. Smith, Y. Chen, Y. Ma, M. Kippax-Jones, M. Fan, W. Lu, M. D. Frogley, G. Cinque, S. J. Day, S. P. Thompson, Y. Cheng, L. L. Daemen, A. J. Ramirez-Cuesta, M. Schröder, S. Yang, Structural and Dynamic Analysis of Sulphur Dioxide Adsorption in a Series of Zirconium - Based Metal - Organic Frameworks, *Angew. Chem. Int. Ed.* 2022, **61**, e202207259.
- 17 A. Aijaz, A. Karkamkar, Y. J. Choi, N. Tsumori, E. Rönnebro, T. Autrey, H. Shioyama, Q. Xu, Immobilizing highly catalytically active Pt nanoparticles inside the pores of metal-organic framework: a double solvents approach, *J. Am. Chem. Soc.* 2012, **34**, 13926-13929.
- 18 Y. A. Teterin, A. Y. Teterin, A. M. Lebedev and I. O. Utkin, The XPS spectra of cerium compounds containing oxygen, *J. Electron Spectros. Relat. Phenomena* 1998, **88**, 275-279.
- 19 H. Chen, C. Liu, W. Guo, Z. Wang, Y. Shi, Y. Yu, L. Wu, Functionalized UiO-66 (Ce) for photocatalytic organic transformation: the role of active sites modulated by ligand functionalization, *Catal. Sci. Technol.* 2022, **6**, 1812-1823.
- 20 C. Wang, Y. Jia, Z. Zhang, G. Zhao, Y. Liu, Y. Lu, Role of PdCx species in Pd@ PdCx/AlOOH/Al-fiber catalyst for the CO oxidative coupling to dimethyl oxalate, *Appl. Surf. Sci.* 2019, **478**, 840-845.
- 21 L. Li, Y. Li, L. Jiao, X. Liu, Z. Ma, Y.-J. Zeng, X. Zheng and H.-L. Jiang, Light-induced selective hydrogenation over PdAg nanocages in hollow MOF microenvironment, *J. Am. Chem. Soc.* 2022, **37**, 17075-17085.
- 22 Y. Chen, W. Lu, M. Schröder and S. Yang, Analysis and Refinement of Host-Guest Interactions in Metal-Organic Frameworks, *Acc. Chem. Res.* 2023, **19**, 2569-2581.
- 23 J. Wang, Y. Cao, Q.-W. Meng, Y. Wang, H. Shi, B. Feng, Y. Huang, Q. Sun and L. He, Catalysis of Synergistic Reactions by Host-Guest Assemblies: Reductive Carbonylation of Nitrobenzenes, *JACS Au* 2023, **8**, 2166-2173.
- 24 B. A. Wilhite, M. J. McCready, A. Varma Kinetics of Phenylacetylene Hydrogenation over Pt/ γ -Al₂O₃ Catalyst, *Ind. Eng. Chem. Res.* 2002, **14**, 3345-3350.
- 25 C. Zhang, L. Wu, R. Ye, G. Feng, R. Zhang Promoter Effect on Ni/SiO₂ Catalysts for Acetylene Semi-hydrogenation to Ethylene. *Catal. Lett.* 2024, **154**, 3619-3627.
- 26 D. Wang, R. Ye, C. Zhang, C. Jin, Z. Lu, M. Shakouri, B. Han, T. Wang, Y. Zhang, R. Zhang, Y. Hu, J. Zhou, G. Feng Robust



- NixSn/ZSM-12 Catalysts with Zeolite as the Support and Sn as the Promoter for Acetylene Semi-hydrogenation *Energy & Fuels* 2023, **37**, 13305-13318.
- 27 Y. Gorbanev, N. Stehling, D. O'Connell and V. Chechik, Reactions of nitroxide radicals in aqueous solutions exposed to non-thermal plasma: limitations of spin trapping of the plasma induced species *PSSST*, 2016, **25**, 055017.
- 28 Y. Gorbanev, C. C. W. Verlaack, S. Tinck, E. Tuentner, K. Foubert, P. Cos, A. Bogaerts, Combining experimental and modelling approaches to study the sources of reactive species induced in water by the COST RF plasma jet, *PCCP* 2018, **20**, 2797-2808.

View Article Online
DOI: 10.1039/D4QI02225D

Open Access Article. Published on 31/11/2024. Downloaded on 07/11/2024 11:25:15.
This article is licensed under a Creative Commons Attribution-NonCommercial 3.0 Unported Licence.



Data availabilityView Article Online
DOI: 10.1039/D4QI02225D

All relevant data are available from the corresponding authors (M.Schroder@manchester.ac.uk; Sihai.Yang@pku.edu.cn), and/or are included in the Electronic Supporting Information. The crystallographic data of the structures reported in this work have been deposited in the Cambridge Crystallographic Data Centre (CCDC) under accession numbers CCDC: 2205374 and 2205379. These can be obtained free of charge from CCDC.

